

---

# Feasibility and Image Quality of Dual-Isotope SPECT Using $^{18}\text{F}$ -FDG and $^{99\text{m}}\text{Tc}$ -Tetrofosmin After Acipimox Administration

Boen L.R. Kam, MD<sup>1</sup>; Roelf Valkema, MD, PhD<sup>1</sup>; Don Poldermans, MD, PhD<sup>2,3</sup>; Jeroen J. Bax, MD, PhD<sup>4</sup>; Ambroos E.M. Reijts, MSc<sup>1</sup>; Riccardo Rambaldi, MD, PhD<sup>3</sup>; Eric Boersma, PhD<sup>3</sup>; Trinet Rietveld, BSc<sup>2</sup>; Jos R.T.C. Roelandt, MD, PhD<sup>3</sup>; and Eric P. Krenning, MD, PhD<sup>1,2</sup>

<sup>1</sup>Department of Nuclear Medicine, Erasmus MC, Rotterdam, The Netherlands; <sup>2</sup>Department of Internal Medicine, Erasmus MC, Rotterdam, The Netherlands; <sup>3</sup>Thoraxcentre, Department of Cardiology, Erasmus MC, Rotterdam, The Netherlands; and <sup>4</sup>Department of Cardiology, Leiden University Medical Centre, Leiden, The Netherlands

---

Currently, with the rapidly increasing number of patients with heart failure due to chronic coronary artery disease, the need for viability studies to guide treatment in these patients is increasing. The most accurate method for viability assessment is metabolic imaging with  $^{18}\text{F}$ -FDG with PET or SPECT. To obtain excellent image quality in all patients, the  $^{18}\text{F}$ -FDG studies should be performed during hyperinsulinemic euglycemic clamping. However, this approach is time-consuming and is not feasible in busy nuclear medicine laboratories. Recently, the use of a nicotinic acid derivative, acipimox, has been suggested, but limited data are available on the image quality of the  $^{18}\text{F}$ -FDG studies using this approach. **Methods:** We evaluated the feasibility and image quality of  $^{18}\text{F}$ -FDG SPECT (with dual-isotope simultaneous acquisition (DISA) using  $^{99\text{m}}\text{Tc}$ -tetrofosmin to assess perfusion) after acipimox administration in 50 nondiabetic patients. The image quality of both  $^{18}\text{F}$ -FDG and  $^{99\text{m}}\text{Tc}$ -tetrofosmin was assessed visually and quantitatively using myocardium-to-blood-pool (M/B) ratios as a measure of target-to-background ratio. The image quality and diagnostic value of DISA  $^{99\text{m}}\text{Tc}$ -tetrofosmin SPECT was compared with standard  $^{99\text{m}}\text{Tc}$ -tetrofosmin SPECT at baseline. **Results:** After acipimox administration, the plasma levels of free fatty acids were extremely low ( $68 \pm 89$  nmol/L). No severe side effects were observed, only paroxysmal flushing. The  $^{18}\text{F}$ -FDG image quality was good in 46 patients (92%) and moderate but still interpretable in the other 4 patients (8%). The clinical information of the baseline  $^{99\text{m}}\text{Tc}$ -tetrofosmin SPECT was retained in the DISA  $^{99\text{m}}\text{Tc}$ -tetrofosmin SPECT images because we did observe no substantial fill-in of perfusion defects by high  $^{18}\text{F}$ -FDG uptake in the same segment. **Conclusion:** Cardiac  $^{18}\text{F}$ -FDG SPECT after acipimox is safe and resulted consistently in good image quality; this simple approach may be the method of choice for routine cardiac metabolic imaging.

**Key Words:**  $^{18}\text{F}$ -FDG;  $^{99\text{m}}\text{Tc}$ -tetrofosmin; SPECT; myocardial viability; image quality

**J Nucl Med 2003; 44:140–145**

**H**heart failure secondary to coronary artery disease is an important clinical problem (1). Patients with myocardial viability and impaired left ventricular function may benefit from coronary revascularization because improvement of function and long-term prognosis may be anticipated (2). Myocardial viability can be assessed with many techniques (3); among these techniques, metabolic imaging with  $^{18}\text{F}$ -FDG and PET is considered the most accurate method to assess viability and has been demonstrated to adequately predict functional recovery after revascularization (4–6). SPECT with high-energy collimators has been used successfully for myocardial  $^{18}\text{F}$ -FDG imaging and has the advantage of wider availability, making routine use possible (7–10). Earlier studies used sequential perfusion imaging (using  $^{201}\text{Tl}$ ) and  $^{18}\text{F}$ -FDG SPECT for assessment of viability (10). To improve patient throughput, several groups have reported the use of dual-isotope simultaneous acquisition (DISA) SPECT using  $^{99\text{m}}\text{Tc}$ -sestamibi (to assess perfusion) together with  $^{18}\text{F}$ -FDG (7–9).

An essential aspect of cardiac  $^{18}\text{F}$ -FDG imaging is the metabolic preparation of the patient to stimulate  $^{18}\text{F}$ -FDG uptake in the heart. Oral glucose uptake will often result in suboptimal  $^{18}\text{F}$ -FDG uptake (11) and the hyperinsulinemic euglycemic clamp technique (12) is rather time-consuming. The use of nicotinic acid derivatives, such as acipimox, to lower serum levels of free fatty acids (FFAs), and thereby enhance cardiac glucose and  $^{18}\text{F}$ -FDG uptake, may be an attractive alternative. However, the image quality of cardiac  $^{18}\text{F}$ -FDG studies using this approach has been studied only in small patient groups (13,14).

This study evaluated the feasibility of DISA SPECT using  $^{99\text{m}}\text{Tc}$ -tetrofosmin and  $^{18}\text{F}$ -FDG after administration of acipimox in 50 nondiabetic patients with chronic coronary artery disease and impaired left ventricular function. Comparison of DISA SPECT with normal  $^{99\text{m}}\text{Tc}$ -tetrofosmin imaging was done to determine possible image degradation due to 511-keV downscatter. This study also evalu-

---

Received Feb. 25, 2002; revision accepted Sep. 25, 2002.  
For correspondence contact: Roelf Valkema, MD, PhD, Department of Nuclear Medicine, L208, Erasmus MC, P.O. Box 2040, 3000 CA Rotterdam, The Netherlands.  
E-mail: valkema@nuge.azr.nl

ated the incidence of viable myocardium in dyskinetic and akinetic segments as assessed by echocardiography.

## MATERIALS AND METHODS

### Patients

Fifty patients (42 men, 8 women; mean age,  $55 \pm 19$  y) were included in the study. They had a history of chronic coronary artery disease (determined by coronary angiography): 7 had 1-vessel, 12 had 2-vessel, and 31 had 3-vessel disease. The mean left ventricular ejection fraction was  $32\% \pm 10\%$  determined by radionuclide ventriculography. All had a previous myocardial infarction (>6 mo before the study). Patients with diabetes mellitus or impaired glucose tolerance were excluded.

All patients underwent 2-dimensional (2D) echocardiography (to identify regions of contractile dysfunction) followed by DISA SPECT after oral administration of acipimox.

### Resting 2D Echocardiography

For the assessment of contractile function, all patients underwent resting 2D echocardiography. This was performed using a Sonos-5500 imaging system (Hewlett Packard, Palo Alto, CA) with harmonic imaging to optimize endocardial border visualization. Standard parasternal long- and short-axis slices were obtained as well as apical long-axis 2- and 4-chamber views as described by the American Society of Echocardiography (15). For analysis, the left ventricle was divided into 16 segments and visually scored by 2 experienced observers (Fig. 1). A 5-point scoring system (1 = normokinesia, 2 = mild hypokinesia, 3 = severe hypokinesia, 4 =

akinesia, and 5 = dyskinesia) was used. Segments with normal wall motion or mild hypokinesia (showing wall thickening) were considered normal. Segments with severe hypokinesia, akinesia, or dyskinesia (scores 3, 4, or 5) were considered dysfunctional.

### Study Design for DISA SPECT

For optimal  $^{18}\text{F}$ -FDG uptake in the heart the patients were asked to remain on a low-fat diet 24 h before the study. On the day of the study the patients were allowed to have a light breakfast. One hour after intravenous injection of 600 MBq  $^{99\text{m}}\text{Tc}$ -tetrofosmin, standard SPECT imaging using low-energy collimators was performed. The patients received orally  $2 \times 250$  mg 5-methylpyrazine-2-carboxylic acid 4-oxide (brand name, Nedios; generic name, acipimox; Byk, Zwanenburg, The Netherlands). The first capsule of 250-mg acipimox was given immediately before the start of standard  $^{99\text{m}}\text{Tc}$ -tetrofosmin SPECT acquisition; the second capsule was given immediately after completion of this acquisition. This schedule was chosen to ensure sufficiently low serum FFA levels at the time of the  $^{18}\text{F}$ -FDG injection and to keep the serum FFA long enough at a low level during the  $^{18}\text{F}$ -FDG accumulation period. Thirty minutes after standard  $^{99\text{m}}\text{Tc}$ -tetrofosmin SPECT, the patients had a light carbohydrate-rich meal to stimulate insulin release, to further improve the  $^{18}\text{F}$ -FDG uptake in the heart. One hour later the patients were injected with 185 MBq  $^{18}\text{F}$ -FDG. After another 45 min, DISA SPECT followed. Serum glucose and FFA levels were determined at baseline (before injection of  $^{99\text{m}}\text{Tc}$ -tetrofosmin) and immediately before the injection of  $^{18}\text{F}$ -FDG.

### Image Acquisition

A triple-head SPECT camera (Prism 3000-XP; Marconi Medical Systems, Cleveland OH) was used. The baseline perfusion SPECT was performed in a standard fashion using low-energy, high-resolution collimators;  $360^\circ$  rotation; 120 views in step-and-shoot mode; 30 s per view. A low-pass filter with order 3.8 and cutoff 0.19 cycles per pixel was used, followed by reorientation in short, vertical and horizontal long-axis slices of 7.7-mm thickness. DISA SPECT was performed with a 15% window around the photopeak for  $^{99\text{m}}\text{Tc}$ -tetrofosmin (140 keV) and a 30% window around the photo peak (511 keV) for  $^{18}\text{F}$ -FDG, using ultra-high-energy collimators (16); 4 acquisitions of 8 min each over  $360^\circ$  in continuous mode and rebinned to 120 views were added to compensate for increasing  $^{18}\text{F}$ -FDG accumulation and  $^{18}\text{F}$  physical decay during the acquisition. A low-pass filter with order 3.5 and cutoff 0.19 cycles per pixel was used for the 140-keV window and cutoff 0.16 cycle per pixel for the 511-keV window. After filtering, reorientation in standard views was done in batch mode to ensure identical orientation for both windows.

### Image Analysis

**Assessment of Image Quality.** The image quality of baseline  $^{99\text{m}}\text{Tc}$ -tetrofosmin, DISA- $^{99\text{m}}\text{Tc}$ -tetrofosmin and DISA- $^{18}\text{F}$ -FDG was classified visually in 3 grades by 2 independent observers: good, moderate, and uninterpretable. Also noted was whether infradiaphragmatic radioactivity was observed, mainly in the bowel lumen, and whether this interfered with the evaluation of the scan.

For quantitative analysis, the image quality was expressed as the myocardial-to-blood-pool (M/B) ratio, which is used as a measure of the target-to-background ratio. The M/B ratio was calculated from a midventricular short-axis slice (both for the DISA  $^{99\text{m}}\text{Tc}$ -tetrofosmin and the DISA  $^{18}\text{F}$ -FDG short-axis slices). A small

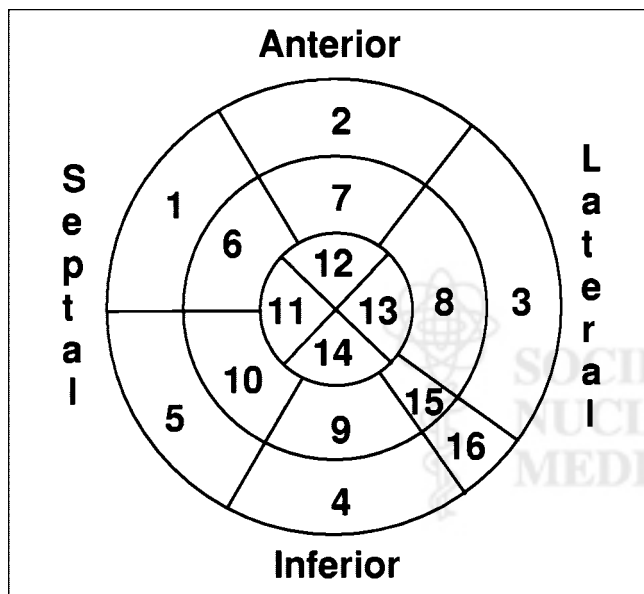


**FIGURE 1.** Segmentation of myocardium as used for 2D echocardiography,  $^{18}\text{F}$ -FDG, and  $^{99\text{m}}\text{Tc}$ -tetrofosmin DISA SPECT. Conventional echocardiography segments (15) are plotted in polar map with apex centrally and basal segments in outer ring. This format was used to enable optimal comparison between 2D echocardiography and SPECT. Vascular territories are indicative only and may differ between patients (segments 1, 2, 6, 7, and 10–14 represent left anterior descending coronary artery; segments 3, 8, 13, 15, and 16 represent left circumflex coronary artery; and segments 4, 5, 9, and 14 represent right coronary artery).

region of interest (ROI) comprising 30 pixels was drawn over a segment with normal wall motion (as assessed by 2D echocardiography) and normal perfusion (as assessed by DISA  $^{99m}\text{Tc}$ -tetrofosmin), and a similar ROI was drawn in the center of the blood pool (left ventricular cavity). The myocardial and blood-pool activities were calculated and the M/B ratio (for DISA  $^{99m}\text{Tc}$ -tetrofosmin and DISA  $^{18}\text{F}$ -FDG) was assessed by dividing the myocardial activity by the blood-pool activity.

**Assessment of Viability.** Visual semiquantitative analysis was performed using the same 16-segment model corresponding to echocardiography to enable direct comparison of the same segments (Fig. 1). In segments with contractile dysfunction (see above),  $^{99m}\text{Tc}$ -tetrofosmin and  $^{18}\text{F}$ -FDG uptake were scored semiquantitatively (using quantitative color-coded scales) in 5 grades: 0 = normal tracer uptake (100%–85% activity), 1 = mildly reduced tracer uptake (85%–70% activity), 2 = moderately reduced tracer uptake (70%–50% tracer uptake), 3 = severely reduced tracer uptake (50%–30% activity), and 4 = absent tracer uptake (<30% activity). Dysfunctional segments were considered viable if the perfusion score was 0 or 1 (normal perfusion) or if the  $^{18}\text{F}$ -FDG uptake score was higher than the  $^{99m}\text{Tc}$ -tetrofosmin uptake score (perfusion– $^{18}\text{F}$ -FDG mismatch pattern). Dysfunctional segments were considered scar tissue when a perfusion defect (score 2 or more) exhibited concordantly reduced  $^{18}\text{F}$ -FDG uptake (match pattern). To classify a patient as viable, the presence of 4 or more dysfunctional but viable segments was required.

**DISA Influence on Perfusion.** The spillover from scattered 511-keV photons in the 140-keV  $^{99m}\text{Tc}$  energy window may potentially obscure perfusion defects. For the evaluation of possible spillover, all DISA  $^{99m}\text{Tc}$ -tetrofosmin scans were compared with the baseline  $^{99m}\text{Tc}$ -tetrofosmin scans, also using the 16-segment model. This is only clinically relevant in segments with perfusion defects because normally perfused myocardium is considered to be viable. The perfusion defect scores of baseline and corresponding DISA  $^{99m}\text{Tc}$ -tetrofosmin segments were scored. Because the diminished defect with DISA could be caused by spillover from the 511-keV photons,  $^{18}\text{F}$ -FDG mismatch in those regions was also scored.

### Statistics

All results are expressed as mean  $\pm$  SD. Patient data were compared using the Student *t* test for paired and unpaired data when appropriate.  $P < 0.05$  was considered significant.

### RESULTS

The plasma glucose levels at baseline and at the time of  $^{18}\text{F}$ -FDG injection were within the normal range in all individuals ( $5.2 \pm 0.8$  mmol/L). The mean serum FFA levels decreased sharply from  $393 \pm 217$  to  $68 \pm 89$  nmol/L ( $P < 0.001$ ) after an oral dose of  $2 \times 250$  mg acipimox as shown in Figure 2. The reason for the serum increase in 1 patient is unknown. Most of the patients had no side effects; facial flushes were seen occasionally.

The image quality scores are displayed in Figure 3. The quality of the DISA  $^{99m}\text{Tc}$ -tetrofosmin study was good in 47 patients (94%) and moderate in 3; none had uninterpretable images. In 8 cases (16%) there was interfering bowel activity, whereas in 31 of the DISA  $^{99m}\text{Tc}$ -tetrofosmin cases noninterfering bowel activity was observed. These scores were close to the scores of the baseline  $^{99m}\text{Tc}$ -tetrofosmin

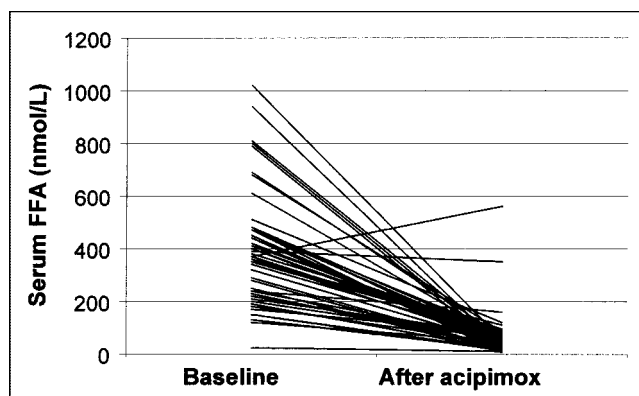


**FIGURE 2.** Serum FFAs before and after  $2 \times 250$  mg acipimox orally. Decrease is highly significant ( $P < 0.001$ ; paired *t* test).

SPECT images: 50 cases (100%) with good quality, 39 with (78%) noninterfering bowel activity, and 5 with (10%) interfering bowel activity.

The quality of the DISA  $^{18}\text{F}$ -FDG images was good in 46 patients (92%) and moderate in 4 (8%); none had uninterpretable images. Interfering bowel activity was observed in only 2 cases (4%).

An example of the image quality of the DISA  $^{99m}\text{Tc}$ -tetrofosmin and the DISA  $^{18}\text{F}$ -FDG images is shown in Figure 4.

The mean total counts in the short-axis ROIs (in normal myocardium) were  $1,912 \pm 703$  for DISA  $^{18}\text{F}$ -FDG and  $2,827 \pm 833$  for DISA  $^{99m}\text{Tc}$ -tetrofosmin. The M/B ratios were  $3.83 \pm 1.31$  for DISA  $^{18}\text{F}$ -FDG and  $8.00 \pm 8.39$  for DISA  $^{99m}\text{Tc}$ -tetrofosmin.

On resting 2D echocardiography, 349 segments (44%) exhibited dysfunction. Of these 349 dysfunctional segments, 108 (31%) were classified as viable: 89 (82%) showed normal perfusion and 19 (18%) had a perfusion  $^{18}\text{F}$ -FDG mismatch. Scar tissue was present in 241 segments (69%) (showing a perfusion  $^{18}\text{F}$ -FDG match). On a patient basis (defined as 4 or more dysfunctional segments being viable, representing  $\geq 25\%$  of the left ventricle), 11 patients (22%) were classified as viable, and 39 (78%) were classified as nonviable.

Comparison between baseline  $^{99m}\text{Tc}$ -tetrofosmin and DISA  $^{99m}\text{Tc}$ -tetrofosmin showed that 444 of 800 segments scored a grade 2 defect or worse on the baseline scan. In segments with perfusion–metabolism mismatch the perfusion defect score was at least as high with DISA as at baseline. In 9 of these 444 segments (5%), the defect score on the DISA was less than that on the baseline study. Conversely, in 5 of the 444 segments (1%), the DISA perfusion defect score was worse than that at baseline. However, none of these segments showed  $^{18}\text{F}$ -FDG–tetrofosmin mismatch. Therefore, we observed no fill-in of the perfusion image by spillover from high  $^{18}\text{F}$ -FDG activity. In none of the patients was the clinical judgment different whether the baseline perfusion or the DISA image was used.

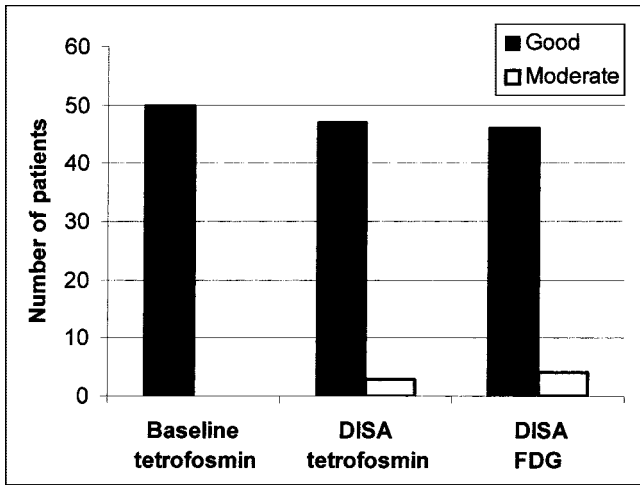


**FIGURE 3.** Image quality scores of baseline <sup>99m</sup>Tc-tetrofosmin, DISA <sup>99m</sup>Tc-tetrofosmin, and DISA <sup>18</sup>F-FDG images.

## DISCUSSION

The number of patients with heart failure due to coronary artery disease is increasing rapidly (1). These patients require much medical care, generating high costs. Myocardial viability assessment by <sup>18</sup>F-FDG PET is clinically important in these patients, but limited availability of PET cameras hampers application of <sup>18</sup>F-FDG imaging on a large scale. Over the past 10 y, much effort has been invested in the development of high-energy SPECT imaging (7–10): at first, using sequential perfusion (mainly with <sup>201</sup>Tl as a perfusion agent) and <sup>18</sup>F-FDG imaging and, more recently, using DISA perfusion–<sup>18</sup>F-FDG protocols (10). Sandler et al. (8) and Delbeke et al. (9) have reported the use of DISA SPECT with <sup>99m</sup>Tc-sestamibi and <sup>18</sup>F-FDG and in this study <sup>99m</sup>Tc-tetrofosmin was used, yielding excellent image quality. DISA SPECT has the advantage of reducing imaging time compared with sequential perfusion–<sup>18</sup>F-FDG imaging and, thus, potentially increasing patient throughput. Be-

sides, DISA SPECT allows perfect alignment of the perfusion and <sup>18</sup>F-FDG images. However, DISA SPECT was still impractical for routine cardiac <sup>18</sup>F-FDG imaging because hyperinsulinemic euglycemic clamping was still needed to ensure adequate image quality in all patients (12); previous data have demonstrated that oral glucose loading may result in poor image quality in up to 30% of the patients (11). Although hyperinsulinemic euglycemic clamping yields excellent <sup>18</sup>F-FDG image quality, the procedure is laborious and time-consuming. The rationale of the clamping procedure is to ensure high insulin levels and low FFA levels. Under these circumstances, cardiac glucose (and, thus, <sup>18</sup>F-FDG) uptake is excellent. In the presence of low FFA levels, the myocardium switches from FFA utilization to glucose utilization (the Randle cycle) (17), and the high insulin levels stimulate cardiac glucose uptake directly and indirectly (by inhibition of peripheral lipolysis). Previous studies have demonstrated excellent image quality using the hyperinsulinemic euglycemic clamp. Recently, 2 studies (one with 8 patients, the other with 15 patients) have demonstrated the feasibility of cardiac <sup>18</sup>F-FDG studies using a nicotinic acid derivative, acipimox (13,14). Acipimox lowers FFA levels by inhibition of lipolysis. In this study, the mean FFA levels after acipimox administration were reduced to extremely low values ( $68 \pm 89$  nmol/L) at the time of <sup>18</sup>F-FDG injection, resulting in predominantly glucose (and <sup>18</sup>F-FDG) utilization of the myocardium. Besides, the addition of a light carbohydrate-rich meal results in enhanced insulin levels as demonstrated previously (14). Thus, theoretically, acipimox administration in combination with a light meal should result in adequate <sup>18</sup>F-FDG image quality. Currently, few data are available on cardiac <sup>18</sup>F-FDG imaging using acipimox (13,14). In this study, we have demonstrated good image quality in 92% of the patients, whereas 8% of the images were of moderate quality. Importantly, all images were interpretable and, as reflected by the M/B ratios of the <sup>18</sup>F-FDG studies ( $3.83 \pm 1.31$  for

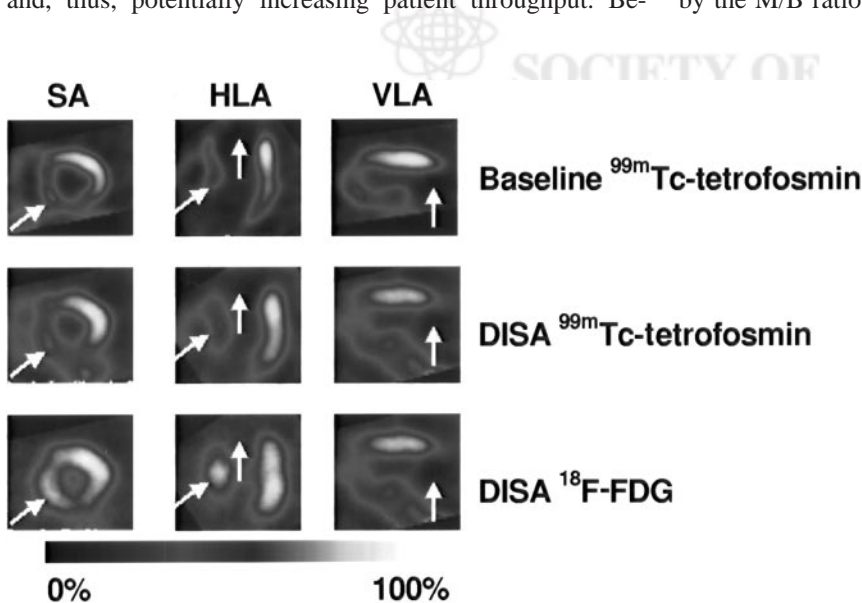


**FIGURE 4.** Baseline <sup>99m</sup>Tc-tetrofosmin, DISA <sup>99m</sup>Tc-tetrofosmin, and DISA <sup>18</sup>F-FDG SPECT images of patient with known 2-vessel disease. (Top row) Baseline <sup>99m</sup>Tc-tetrofosmin short-axis (SA), horizontal long-axis (HLA), and vertical long-axis (VLA) slices. (Center row) Corresponding DISA <sup>99m</sup>Tc-tetrofosmin images. (Bottom row) Corresponding <sup>18</sup>F-FDG slices. There is large severe defect in perfusion and glucose metabolism in area of apex (matched pattern, scar; vertical arrows). In septum, there is moderate perfusion defect with nearly normal glucose metabolism (mismatch pattern, viable; oblique arrows). Additionally, there is mild perfusion defect in basal posterior area with mismatch (best seen on HLA images, no arrows). DISA perfusion images are less sharp than baseline perfusion images, but diagnostic information is retained.

DISA  $^{18}\text{F}$ -FDG), the ratio of target-to-background activities was good and even higher than that reported earlier (14). The  $^{99\text{m}}\text{Tc}$ -tetrofosmin images during DISA were usually less sharp than those using normal low-energy collimators (Fig. 4). However, the clinical information was retained, as we observed no substantial fill-in of perfusion defects by high  $^{18}\text{F}$ -FDG uptake in the same segment. Therefore, the contribution of downscattered 511-keV photons in the 140-keV energy channel as demonstrated by other investigators (7–9) was of no great clinical importance.

$^{18}\text{F}$ -FDG imaging after acipimox administration further simplifies the imaging protocol: Acipimox can be administered orally, without the need for intravenous administration of insulin or glucose. Importantly,  $^{18}\text{F}$ -FDG imaging after acipimox administration is safe; the only side effects were harmless paroxysmal flushing in some patients.

Moreover, in the limited available data, the  $^{18}\text{F}$ -FDG image quality was comparable after acipimox administration and hyperinsulinemic euglycemic clamping (13,14).

An important issue that needs further study is whether acipimox administration results in good image quality in all patients, including patients with insulin resistance or diabetes mellitus, who were excluded from this study.

Still, the present data demonstrate the feasibility of a simple and practical imaging protocol, well suited for clinical routine cardiac  $^{18}\text{F}$ -FDG imaging, without the need for complex infusions. Also, the DISA SPECT protocol shortens acquisition time and allows perfect alignment between perfusion and  $^{18}\text{F}$ -FDG images. We used 2D echocardiography in this study to identify the dysfunctional myocardial segments. Unfortunately, the standard echocardiographic segmentation (15) is different from the usual segmentation models used for myocardial perfusion SPECT. To enable head-to-head comparison of the 2 different methods, we used a new polar view SPECT segmentation as close as possible to the echocardiographic standard. This is not ideal, however, because there is still a chance of misalignment of segments when comparing the 2 different modalities. Additionally, the attributed volume of myocardium is uneven between segments, especially prominent in the apex, which is divided in 4 segments in this model. In the future, gating of the SPECT images may replace the use of 2D echocardiography to identify regions with contractile dysfunction and all information can be derived from a single comprehensive study.

The validation of the viability results of  $^{18}\text{F}$ -FDG DISA SPECT compared with an independent method was beyond the scope of this study. In a larger group of patients, without exclusion of patients with diabetes mellitus or glucose intolerance, we found 81% overall agreement between  $^{18}\text{F}$ -FDG DISA SPECT and dobutamine stress echocardiography in detecting myocardial viability (18). In that analysis a higher prevalence of viability was found with  $^{18}\text{F}$ -FDG DISA SPECT than with dobutamine stress echocardiography. The functional outcome after revascularization will be

the final validation for both techniques; this will be analyzed in the future.

## CONCLUSION

The nicotinic acid derivative acipimox can be used safely and results in good myocardial  $^{18}\text{F}$ -FDG uptake in patients without diabetes mellitus or impaired glucose tolerance. Using inpatient comparison with standard resting perfusion image degradation with DISA SPECT, despite the use of high-energy collimators and the downscatter of 511-keV photons of  $^{18}\text{F}$  in the  $^{99\text{m}}\text{Tc}$  window.  $^{18}\text{F}$ -FDG DISA SPECT with acipimox is a convenient method for cardiac metabolic imaging.

## ACKNOWLEDGMENTS

The authors thank Jacobus W.O. van den Berg, PhD, Department of Internal Medicine, for expert assistance in the analysis of serum FFAs and the technicians and administrative personnel of the Department of Nuclear Medicine for their effort in conducting the scintigraphic studies.

## REFERENCES

1. Gheorghide M, Bonow RO. Chronic heart failure in the United States: a manifestation of coronary artery disease. *Circulation*. 1998;97:282–289.
2. Beller GA. Assessment of myocardial viability. *Curr Opin Cardiol*. 1997;12:459–467.
3. Marwick TH. The viable myocardium: epidemiology, detection, and clinical implications. *Lancet*. 1998;351:815–819.
4. Eitzman D, Al-Aouar Z, Kanter HL, et al. Clinical outcome of patients with advanced coronary artery disease after viability studies with positron emission tomography. *J Am Coll Cardiol*. 1992;20:559–565.
5. DiCarli M, Davidson M, Little R, et al. Value of metabolic imaging with positron emission tomography for evaluating prognosis in patients with coronary disease and left ventricle dysfunction. *Am J Cardiol*. 1994;73:527–533.
6. Tillisch J, Brunken R, Marshall R, et al. Reversibility of cardiac wall-motion abnormalities predicted by positron tomography. *N Engl J Med*. 1986;314:884–888.
7. Stoll H-P, Hellwig N, Alexander C, et al. Myocardial metabolic imaging by means of fluorine-18 deoxyglucose/technetium-99m sestamibi dual-isotope single photon emission tomography. *Eur J Nucl Med*. 1994;21:1085–1093.
8. Sandler MP, Videlefsky S, Delbeke D, et al. Evaluation of myocardial ischemia using a rest metabolism/stress perfusion protocol with fluorine-18 deoxyglucose/technetium-99m MIBI and dual-isotope simultaneous-acquisition single-photon emission computed tomography. *J Am Coll Cardiol*. 1995;26:870–888.
9. Delbeke D, Videlefsky S, Patton JA, et al. Rest myocardial perfusion/metabolism imaging using simultaneous dual isotope acquisition SPECT with technetium-99m-MIBI/fluorine-18-FDG. *J Nucl Med*. 1995;36:2110–2119.
10. Bax JJ, Patton JA, Poldermans D, et al. 18-Fluorodeoxyglucose imaging with PET and SPECT: cardiac applications. *Semin Nucl Med*. 2000;30:281–298.
11. Lee KS, Vom Dahl J, Hicks RJ, et al. Relationship between blood glucose levels and F-18 fluorodeoxyglucose image quality in cardiac FDG PET studies [abstract]. *J Am Coll Cardiol*. 1991;17:120A.
12. Knuuti MJ, Nuutila P, Ruotsalainen U, et al. Euglycemic hyperinsulinemic clamp and oral glucose load in stimulating myocardial glucose utilization during positron emission tomography. *J Nucl Med*. 1992;33:1255–1262.
13. Knuuti MJ, Yki-Jarvinen H, Voipio-Pulkki LM, et al. Enhancement of myocardial [fluorine-18]fluorodeoxyglucose uptake by a nicotinic acid derivative. *J Nucl Med*. 1994;35:989–998.
14. Bax JJ, Veening MA, Visser FC, et al. Optimal metabolic conditions during fluorine-18 fluorodeoxyglucose imaging: a comparative study using different protocols. *Eur J Nucl Med*. 1997;24:35–41.
15. Schiller NB, Shah PM, Crawford M, et al. Recommendation for quantification of the left ventricle by two-dimensional echocardiography. *J Am Soc Echocardiogr*. 1989;2:358–367.

16. Van Lingen A, Huijgens PC, Visser FC, et al. Performance characteristics of a 511 keV collimator for imaging positron emitters with a standard gamma-camera. *Eur J Nucl Med.* 1992;19:315–321.
17. Knuuti MJ, Mäki M, Yki-Järvinen H, et al. The effect of insulin and FFA on the myocardial glucose uptake. *J Mol Cell Cardiol.* 1995;27:1359–1367.
18. Rambaldi R, Poldermans D, Bax JJ, et al. Dobutamine stress echocardiography and technetium-99m-tetrofosmin/fluorine-18-fluorodeoxyglucose single-photon emission computed tomography and influence of resting ejection fraction to assess myocardial viability in patients with severe left ventricular dysfunction and healed myocardial infarction. *Am J Cardiol.* 1999;84:130–134.

### Erratum

In “Quantification of D<sub>2</sub>-Like Dopamine Receptors in the Human Brain with <sup>18</sup>F-Desmethoxyfallypride,” by Gründer et al. (*J Nucl Med.* 2003;44:109–116), the values reported in Table 1 were incorrect. The correct values appear below. The authors regret the error.

**TABLE 1**  
VDs and BPs in Human Brain

Model	Cerebellum	Thalamus	Caudate	Putamen
VD 2-compartment	3.11 ± 0.94	3.83 ± 1.33	8.74 ± 3.00	10.76 ± 3.58
BP 2-compartment*	—	0.22 ± 0.08	1.80 ± 0.41	2.44 ± 0.40
VD 3-compartment	—	3.73 ± 1.41	8.73 ± 3.01	10.74 ± 3.59
BP 3-compartment	—	0.18 ± 0.12	1.79 ± 0.41	2.44 ± 0.40
VD Logan invasive	3.29 ± 0.92	3.92 ± 1.37	8.87 ± 3.00	10.97 ± 3.61
BP Logan invasive*	—	0.18 ± 0.10	1.67 ± 0.37	2.30 ± 0.32
BP Logan noninvasive	0	0.19 ± 0.10	1.61 ± 0.34	2.21 ± 0.31
BP reference tissue	—	0.20 ± 0.07	1.68 ± 0.37	2.33 ± 0.31
BP equilibrium	—	0.22 ± 0.14	1.65 ± 0.22	2.19 ± 0.32

\*Indirect estimate, determined from respective VD.

Logan invasive model = Logan plot with arterial blood sampling; Logan noninvasive method = Logan plot with reference region.